

Supplementary Information

Reverse Intersystem Crossing from High-Level Triplet Excited Electronic States of Fluorescent Organic Molecules

Qianqian Xu,^{*a} Andrew D. Scully,^c Melissa Skidmore,^c Hua Ke,^{*d} Xiaojun Wu,^b Jie Li,^b Zhicheng Zhang,^b Xiaochang Li^b and Kazunori Ueno^{*b}

^a School of Chemistry and Materials Science, East China University of Technology, Nanchang 330013, P. R. China. E-mail: qqx_qx@163.com

^b GuanMat Optoelectronic Materials, Inc., Pingxiang 337000, P. R. China. E-mail: drkayxyzq@yahoo.co.jp

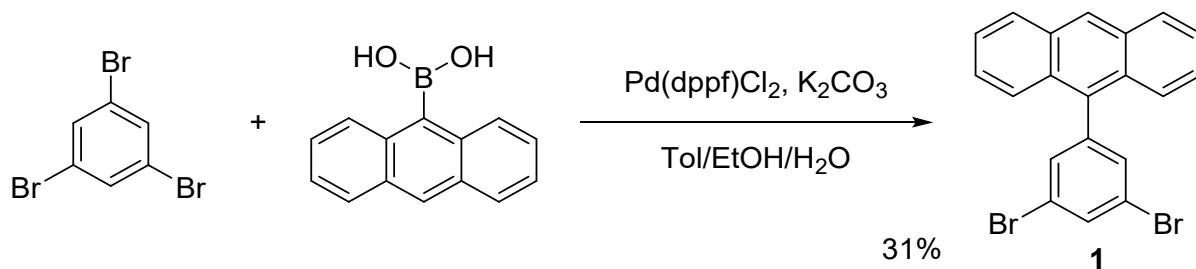
^c CSIRO Manufacturing, Research Way, Clayton, Victoria, 3168, Australia

^d College of Materials and Chemical Engineering, Pingxiang University, Pingxiang, Jiangxi 337055, P. R. China. E-mail: kehua_pxu@163.com

Materials and methods

The ¹H NMR and ¹³C NMR spectra of the following synthesized compounds are shown in Fig. S7- S18.

Synthesis of 1



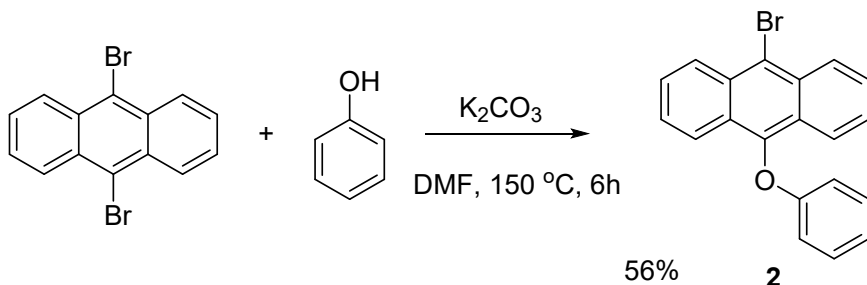
A 2 L flask was charged with 1,3,5-tribromobenzene (20 g, 63.5 mmol), 9-Anthraceneboronic acid (14.1 g, 63.5 mmol), Pd(PPh₃)₄ (1.5 g, 1.3 mmol), K₂CO₃ (18 g, 130.4 mmol), 105 mL toluene, 30 mL ethanol and 65 mL water. The resulting mixture was stirred for 5 h at 100 °C under N₂. Then the reaction mixture was cooled to room temperature and washed with water. The organic solvent was evaporated under reduced pressure. The resulting residue was purified by column chromatography using PE-CH₂Cl₂ (4:1) as an eluent to afford the crude product. The crude product was further purified by being washed with CH₂Cl₂ to afford the product **1** in 31% yield with 98% purity as yellow solid.

MS *m/z* [M]⁺ calc'd for C₂₀H₁₂Br₂: 411.93, found: 412.10.

¹H NMR (400 MHz, Chloroform-d) δ 8.49 (s, 1H), 8.02 (d, *J* = 8.4 Hz, 2H), 7.85 (s, 1H), 7.58 (d, *J* = 8.7 Hz, 2H), 7.52 (s, 2H), 7.46 (dd, *J* = 8.7, 6.2 Hz, 2H), 7.39 (dd, *J* = 8.8, 6.4 Hz, 2H).

¹³C NMR (101 MHz, Chloroform-d) δ 142.65, 133.40, 133.29, 133.02, 131.22, 129.94, 128.56, 127.70, 126.14, 126.04, 125.33, 123.10.

Synthesis of **2**



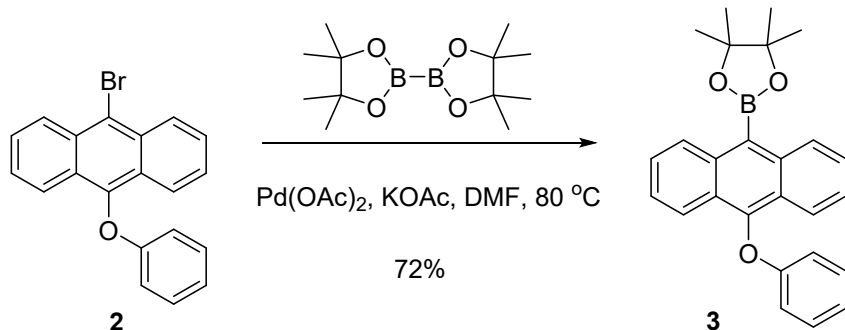
A 50 mL flask was charged with compound 9,10-dibromoanthracene (672 mg, 2.0 mmol), phenol (226 mg, 2.4 mmol), K₂CO₃ (331 mg, 2.4 mmol). 10 mL DMF was added to the flask. The resulting reaction was allowed to proceed for 6 h at 150 °C under N₂. Then the reaction mixture was cooled to room temperature and poured into 100 mL water. The precipitated solid was filtered and purified by column chromatography using petroleum ether (PE) as an eluent to afford the product **2** in 56% yield as yellow solid.

MS *m/z* [M]⁺ calc'd for C₂₀H₁₃BrO: 348.02, found: 348.53.

¹H NMR (400 MHz, Chloroform-d) δ 8.56 (d, J = 8.9 Hz, 2H), 8.11 (d, J = 8.7 Hz, 2H), 7.58 (ddd, J = 8.9, 6.5, 1.2 Hz, 2H), 7.43 (ddd, J = 8.7, 6.5, 1.1 Hz, 2H), 7.28 – 7.14 (m, 2H), 6.98 (t, J = 7.3 Hz, 1H), 6.86 – 6.75 (m, 2H).

¹³C NMR (100 MHz, Chloroform-d) δ 159.94, 145.81, 131.08, 129.79, 127.92, 127.51, 126.15, 125.60, 122.89, 121.97, 118.92, 115.25.

Synthesis of 3



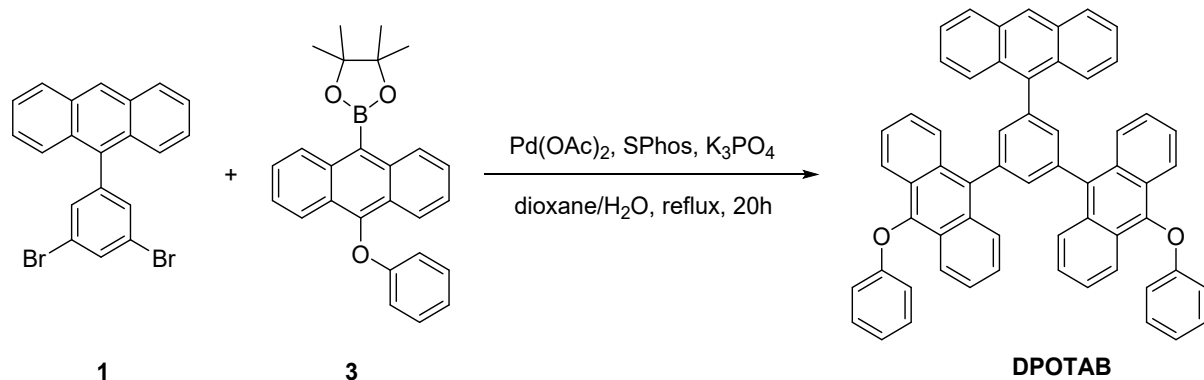
A 250 ml flask was charged with compound **2** (3.49 g, 10 mmol), bis(pinacolato)diboron (3.05 g, 12 mmol), $\text{Pd}(\text{OAc})_2$ (112 mg, 0.5 mmol), KOAc (2.94 g, 30 mmol) and DMF (40 mL). The resulting mixture was stirred for 16 h at $80\text{ }^\circ\text{C}$ under N_2 . Then the reaction mixture was cooled to room temperature and poured into 400 mL water. The resulting mixture was filtered and the residue was purified by column chromatography using PE- CH_2Cl_2 (4:1) as an eluent to afford the product **3** in 72% yield as yellow solid.

MS m/z [M]⁺ calc'd for $\text{C}_{26}\text{H}_{25}\text{BO}_3$: 396.19, found: 396.06.

¹H NMR (400 MHz, Chloroform-d) δ 8.50 (d, J = 9.0 Hz, 2H), 8.12 (d, J = 8.8 Hz, 2H), 7.48 (dd, 2H), 7.38 (dd, J = 8.8, 6.4 Hz, 2H), 7.24 – 7.15 (m, 2H), 6.99 – 6.92 (m, 1H), 6.82 – 6.75 (m, 2H), 1.58 (s, 12H).

¹³C NMR (100 MHz, Chloroform-d) δ 160.14, 147.73, 136.88, 129.74, 128.62, 127.26, 126.19, 125.52, 124.46, 122.87, 121.76, 115.36, 84.56, 25.24.

Synthesis of DPOTAB



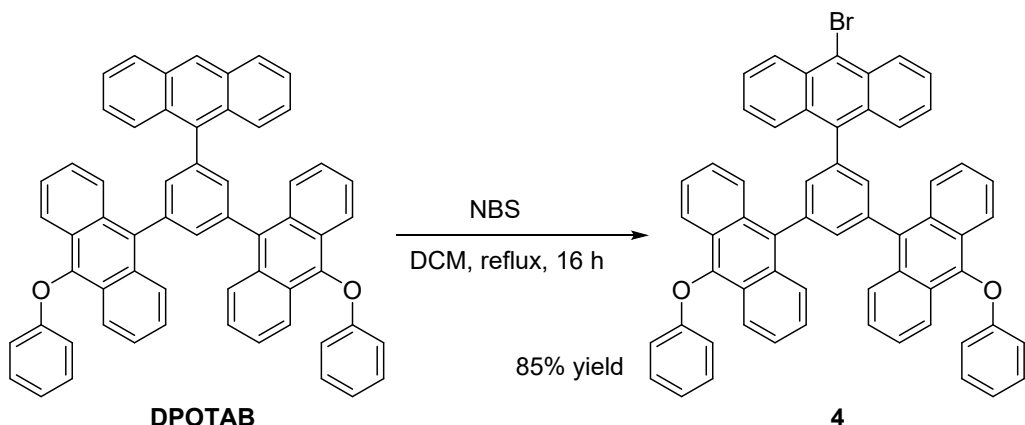
A 250 ml flask was charged with compound **1** (2.551 g, 6.20 mmol), compound **3** (5.885 g, 14.86 mmol), Pd(OAc)_2 (70 mg, 0.31 mmol), SPhos (383 mg, 0.93 mmol), K_3PO_4 (13. 144g, 62 mmol) and 60 ml dioxane- H_2O (5:1). The flask was evacuated and refilled with N_2 for 3 times, and then the reaction mixture was stirred for 24 h under reflux condition. Then the reaction mixture was cooled to room temperature and evaporated under reduced pressure to remove the organic solvent. Then 100 ml water was added to the residue and the resulting mixture was extracted with CH_2Cl_2 (60 ml $\times 3$). The organic layer was combined and evaporated under reduced pressure, and the residue was purified by column chromatography using PE- CH_2Cl_2 (4:1) as an eluent to afford the crude product in 60% yield as yellow solid. The crude product was further purified by vigorously stirring with PE, removing the solvent then vigorously stirring with CH_2Cl_2 . Next, the product was recrystallized with toluene and then recrystallized with DMF to afford the pure product **DPOTAB** in 99.8% purity.

MS m/z [M]⁺ calc'd for $\text{C}_{60}\text{H}_{38}\text{O}_2$: 790.29, found: 790.20.

¹H NMR (400 MHz, Chloroform-d) δ 8.51 (s, 1H), 8.27 – 8.14 (m, 10H), 8.06 (d, J = 8.4 Hz, 2H), 7.87 – 7.81 (m, 3H), 7.56 (dd, J = 8.8, 6.5 Hz, 6H), 7.45 (dd, J = 9.1, 5.8 Hz, 6H), 7.26 – 7.17 (m, 4H), 6.97 (t, J = 7.4 Hz, 2H), 6.85 (d, J = 8.1 Hz, 4H).

¹³C NMR (101 MHz, Chloroform-d) δ 160.21, 145.63, 139.17, 138.85, 136.07, 134.13, 134.02, 133.83, 131.49, 131.07, 130.33, 129.79, 128.67, 127.09, 126.88, 126.56, 126.14, 125.89, 125.70, 125.20, 124.63, 122.76, 121.80, 115.33.

Synthesis of 4



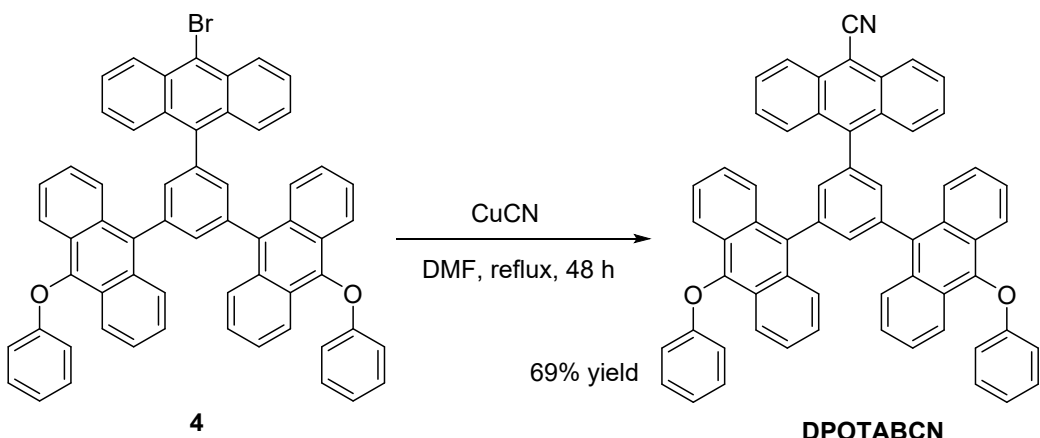
To a stirred solution of DPOTAB (2.96 g, 3.74 mmol) in DCM (12 mL) under reflux was slowly added a DCM solution (8 mL) of NBS (1.665 g, 9.36 mmol), then the reaction was allowed to proceed for 16 h under reflux condition. After the completed, the solvent was removed under reduced pressure, and the resulting residue was purified by silica gel column chromatography (PE/DCM = 5/1) to afford compound **4** 2.76 g in 85% yield as yellowish green solid.

MS m/z [M]⁺ calc'd for C₆₀H₃₇BrO₂: 868.20, found: 867.98.

¹H NMR (400 MHz, Chloroform-d) δ 8.68 – 8.61 (m, 2H), 8.26 – 8.15 (m, 10H), 7.88 (t, J = 1.6 Hz, 1H), 7.81 (d, J = 1.7 Hz, 2H), 7.69 – 7.53 (m, 8H), 7.46 (ddd, J = 8.7, 6.6, 1.1 Hz, 4H), 7.24 – 7.18 (m, 4H), 7.02 – 6.94 (m, 2H), 6.89 – 6.81 (m, 4H).

¹³C NMR (101 MHz, Chloroform-d) δ 160.23, 145.73, 139.00, 138.85, 136.87, 134.52, 133.96, 133.62, 131.16, 131.08, 130.42, 129.87, 128.28, 127.15, 127.13, 126.82, 126.28, 126.20, 125.80, 124.68, 123.36, 122.87, 121.89, 115.38.

Synthesis of DPOTABCN



A 50 ml flask was charged with compound **4** (1.4 g, 1.6 mmol), CuCN (288 mg, 3.2 mmol) and DMF (10 mL), the resulting mixture was stirred at 156 °C under N₂ atmosphere for 48 h. After the reaction completed, the reaction mixture was cooled to room temperature, and poured into 100 mL ice water. Then the precipitate was collected by filtration and purified by silica gel column chromatography (PE/DCM = 3/1) to afford **DPOTABCN** 900 mg in 69% yield as a light green solid.

MS *m/z* [M]⁺ calc'd for C₆₁H₃₇NO₂: 815.28, found: 815.26.

¹H NMR (400 MHz, Chloroform-d) δ 8.57 – 8.48 (m, 2H), 8.27 (dt, *J* = 8.7, 1.1 Hz, 2H), 8.22 – 8.16 (m, 8H), 7.92 (t, *J* = 1.6 Hz, 1H), 7.80 (d, *J* = 1.6 Hz, 2H), 7.76 (ddd, *J* = 8.6, 6.6, 1.2 Hz, 2H), 7.69 (ddd, *J* = 8.8, 6.7, 1.3 Hz, 2H), 7.58 (ddd, *J* = 8.7, 6.6, 1.3 Hz, 4H), 7.46 (ddd, *J* = 8.9, 6.6, 1.1 Hz, 4H), 7.27 – 7.17 (m, 4H), 7.02 – 6.94 (m, 2H), 6.89 – 6.80 (m, 4H).

¹³C NMR (101 MHz, Chloroform-d) δ 160.20, 145.87, 142.83, 139.25, 137.79, 135.02, 133.45, 133.25, 133.21, 131.06, 129.88, 129.79, 128.85, 127.57, 126.91, 126.64, 126.40, 125.88, 125.84, 124.67, 122.95, 121.94, 117.56, 115.36, 106.16.

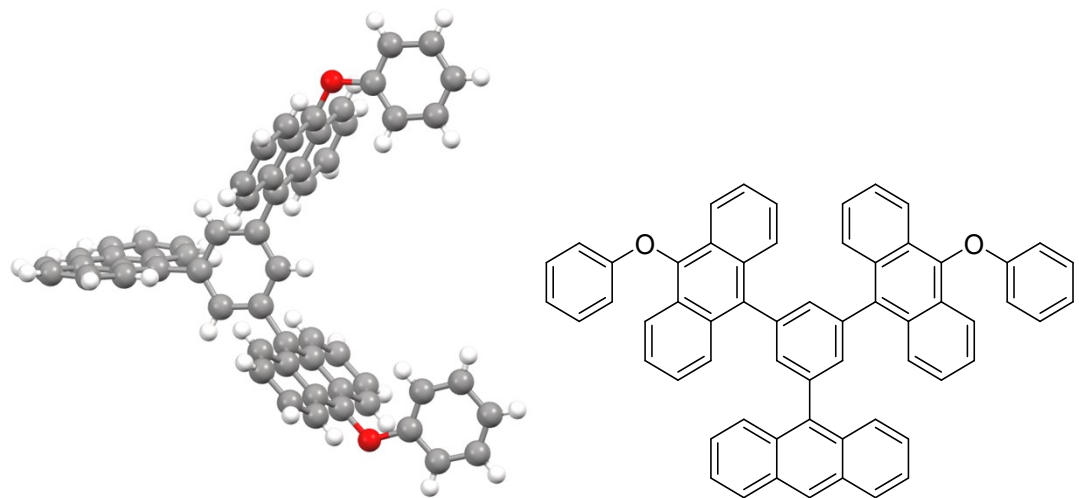


Figure S1. Single Crystal X-Ray Diffraction of DPOTAB (CCDC: 2294880).

Crystal structure determination of DPOTAB

Crystal Data for C₆₀H₃₈O₂ ($M = 790.90$ g/mol): triclinic, space group P-1 (no. 2), $a = 10.7846(2)$ Å, $b = 16.2789(4)$ Å, $c = 16.8851(4)$ Å, $\alpha = 104.238(2)^\circ$, $\beta = 104.743(2)^\circ$, $\gamma = 95.002(2)^\circ$, $V = 2743.02(12)$ Å³, $Z = 2$, $T = 293(2)$ K, $\mu(\text{CuK}\alpha) = 0.439$ mm⁻¹, $D_{\text{calc}} = 0.958$ g/cm³, 36433 reflections measured ($5.634^\circ \leq 2\Theta \leq 150.206^\circ$), 10880 unique ($R_{\text{int}} = 0.0513$, $R_{\text{sigma}} = 0.0540$) which were used in all calculations. The final R_1 was 0.1976 ($I > 2\sigma(I)$) and wR_2 was 0.5173 (all data).

Table S1. Crystal data and structure refinement for DPOTAB

Identification code	DPOTAB
Empirical formula	C ₆₀ H ₃₈ O ₂
Formula weight	790.90
Temperature/K	293(2)
Crystal system	triclinic
Space group	P-1
a/Å	10.7846(2)
b/Å	16.2789(4)
c/Å	16.8851(4)
α/°	104.238(2)
β/°	104.743(2)
γ/°	95.002(2)
Volume/Å ³	2743.02(12)
Z	2
ρ _{calc} g/cm ³	0.958
μ/mm ⁻¹	0.439
F(000)	828.0
Radiation	CuKα ($\lambda = 1.54184$)
2Θ range for data collection/°	5.634 to 150.206
Index ranges	-13 ≤ h ≤ 12, -20 ≤ k ≤ 20, -19 ≤ l ≤ 21
Reflections collected	36433
Independent reflections	10880 [R _{int} = 0.0513, R _{sigma} = 0.0540]
Data/restraints/parameters	10880/0/559
Goodness-of-fit on F ²	1.909
Final R indexes [I>=2σ (I)]	R ₁ = 0.1976, wR ₂ = 0.4492
Final R indexes [all data]	R ₁ = 0.2422, wR ₂ = 0.5173
Largest diff. peak/hole / e Å ⁻³	1.14/-0.59

Table S2. Fractional Atomic Coordinates ($\times 10^4$) and Equivalent Isotropic Displacement Parameters ($\text{\AA}^2 \times 10^3$) for DPOTAB. U_{eq} is defined as 1/3 of the trace of the orthogonalized U_{IJ} tensor.

Atom	x	y	z	U(eq)
C34	1520(4)	1078(3)	322(3)	49.9(10)
C29	867(4)	582(3)	-539(3)	50.1(10)
C21	896(4)	1690(3)	753(2)	48.0(9)
C28	-352(4)	710(3)	-920(2)	51.5(10)
O52	6036(4)	6657(3)	2266(2)	81.1(12)
C15	1626(4)	2300(3)	1602(2)	50.5(10)
C27	-1016(4)	1288(3)	-501(3)	53.1(10)
C22	-372(4)	1782(3)	363(3)	51.7(10)
C4	3849(5)	4439(3)	2356(3)	56.8(12)
O35	-988(4)	229(3)	-1761(2)	71.1(10)
C5	5158(5)	4439(3)	2354(2)	56.1(11)
C18	2356(4)	3048(3)	1607(3)	53.7(11)
C33	2796(5)	946(4)	698(3)	61.4(12)
C17	3056(5)	3644(3)	2361(3)	55.2(11)
C43	2273(6)	2633(4)	3986(3)	68.4(14)
C10	5886(5)	5199(4)	2308(3)	61.9(13)
C11	5304(6)	5920(4)	2292(3)	67.4(15)
C23	-1065(5)	2364(4)	782(3)	66.9(13)
C30	1532(5)	-24(3)	-974(3)	64.7(13)
C56	3034(5)	3495(3)	3132(3)	61.2(12)
C19	2291(5)	2745(3)	3140(2)	58.5(12)
C31	2741(6)	-118(4)	-575(4)	76.1(15)
C6	5783(6)	3713(4)	2387(3)	69.9(14)
C54	6574(6)	7575(4)	1501(4)	75.5(15)
C32	3379(6)	360(4)	261(4)	76.6(15)
C53	5922(5)	6801(3)	1474(3)	62.2(12)
C12	4023(6)	5950(4)	2316(3)	67.7(13)
C3	3300(5)	5184(3)	2362(3)	62.5(12)
C26	-2291(5)	1405(4)	-901(3)	73.2(14)

C59	5162(5)	6454(4)	-27(3)	67.4(13)
C57	6490(6)	7776(5)	737(5)	88.7(19)
C60	5213(5)	6231(4)	718(3)	65.2(13)
C58	5803(6)	7214(5)	-13(4)	79.4(17)
C24	-2298(7)	2447(5)	377(4)	87.8(18)
C44	1382(6)	3026(5)	4390(3)	80.9(18)
C25	-2902(6)	1967(5)	-472(4)	85.8(18)
C2	1986(7)	5223(5)	2380(5)	88.0(18)
C48	3197(7)	2231(5)	4425(3)	83.1(18)
C9	7198(6)	5165(5)	2268(4)	82.1(18)
C37	-145(7)	1335(5)	-2317(4)	85.8(17)
C46	2269(8)	2548(6)	5631(4)	99(2)
C7	7033(6)	3720(5)	2357(4)	89.0(18)
C8	7737(6)	4459(6)	2286(5)	97(2)
C36	-935(6)	609(4)	-2411(3)	75.8(16)
C13	3445(9)	6700(4)	2316(5)	94(2)
C47	3126(9)	2181(5)	5275(4)	104(2)
C16	1617(5)	2138(3)	2372(3)	56.3(11)
C45	1417(8)	2937(6)	5214(4)	100(2)
C39	-1781(8)	183(7)	-3203(4)	116(3)
C51	468(12)	3381(9)	5605(6)	153(5)
C38	-94(10)	1682(7)	-2959(5)	119(3)
C1	1474(9)	5951(6)	2370(6)	111(2)
C14	2203(11)	6695(6)	2355(6)	119(3)
C49	492(9)	3477(7)	4012(5)	119(3)
C40	-1782(15)	509(11)	-3868(6)	160(5)
C50	-371(16)	3857(13)	4409(7)	204(8)
C70	5031(17)	1460(13)	5362(8)	210(9)
C20	4120(10)	1896(7)	4103(5)	123(3)
C41	4127(14)	1761(10)	5713(7)	161(5)
C42	-986(16)	1245(12)	-3766(7)	163(6)
C52	-318(17)	3838(15)	5208(8)	222(9)
C55	5029(15)	1500(13)	4570(8)	194(7)

Table S3. Anisotropic Displacement Parameters ($\text{\AA}^2 \times 10^3$) for DPOTAB. The Anisotropic displacement factor exponent takes the form: $-2\pi^2[h^2a^*{}^2U_{11} + 2hka^*b^*U_{12} + \dots]$.

Atom	U_{11}	U_{22}	U_{33}	U_{23}	U_{13}	U_{12}
C34	51(2)	55(2)	44(2)	14.1(18)	16.3(17)	-3.5(18)
C29	57(2)	50(2)	42(2)	7.2(17)	19.9(18)	-2.4(18)
C21	50(2)	54(2)	36.6(19)	8.8(17)	12.8(17)	-4.6(18)
C28	56(2)	55(3)	32.7(18)	7.2(17)	5.3(17)	-8.1(19)
O52	115(3)	68(2)	43.2(17)	12.8(15)	11.9(18)	-35(2)
C15	50(2)	59(3)	34.7(19)	8.9(17)	7.7(16)	-6.7(18)
C27	52(2)	56(3)	45(2)	12.8(19)	7.9(18)	1.9(19)
C22	60(3)	54(3)	38(2)	12.6(18)	10.5(18)	1.5(19)
C4	71(3)	59(3)	35(2)	8.7(18)	18.0(19)	-12(2)
O35	79(2)	74(2)	45.1(17)	0.0(15)	12.8(15)	-1.7(18)
C5	64(3)	64(3)	32.1(19)	6.7(18)	13.3(18)	-9(2)
C18	65(3)	54(3)	37.6(19)	9.7(17)	17.3(18)	-10(2)
C33	52(2)	74(3)	57(3)	18(2)	16(2)	1(2)
C17	68(3)	54(3)	42(2)	13.0(18)	20.6(19)	-8(2)
C43	85(3)	76(3)	35(2)	17(2)	11(2)	-15(3)
C10	68(3)	70(3)	37(2)	14(2)	7.0(19)	-16(2)
C11	92(4)	62(3)	38(2)	7(2)	19(2)	-25(3)
C23	76(3)	68(3)	54(3)	7(2)	20(2)	21(3)
C30	74(3)	59(3)	61(3)	6(2)	31(2)	2(2)
C56	76(3)	61(3)	36(2)	8.0(18)	13.0(19)	-19(2)
C19	70(3)	66(3)	31.6(19)	13.1(18)	9.1(18)	-13(2)
C31	79(4)	75(4)	85(4)	15(3)	46(3)	19(3)
C6	76(3)	75(4)	53(3)	12(2)	17(2)	4(3)
C54	77(3)	77(4)	64(3)	25(3)	12(2)	-25(3)
C32	57(3)	95(4)	80(4)	21(3)	26(3)	16(3)
C53	72(3)	66(3)	48(2)	19(2)	17(2)	-8(2)
C12	92(4)	61(3)	46(2)	14(2)	18(2)	-2(3)
C3	75(3)	64(3)	49(2)	13(2)	24(2)	-1(2)
C26	65(3)	90(4)	54(3)	20(3)	-1(2)	13(3)

C59	71(3)	85(4)	44(2)	16(2)	14(2)	7(3)
C57	87(4)	91(4)	98(5)	43(4)	38(4)	-13(3)
C60	77(3)	62(3)	52(2)	13(2)	19(2)	-3(2)
C58	79(4)	105(5)	76(4)	44(3)	41(3)	16(3)
C24	84(4)	94(5)	85(4)	18(3)	24(3)	37(4)
C44	93(4)	101(5)	43(3)	22(3)	18(3)	-11(3)
C25	67(3)	113(5)	73(4)	19(3)	11(3)	35(3)
C2	91(4)	85(4)	96(4)	27(4)	42(4)	7(4)
C48	100(4)	94(4)	41(3)	12(3)	7(3)	-3(4)
C9	67(3)	106(5)	69(3)	25(3)	22(3)	-15(3)
C37	102(5)	96(5)	59(3)	22(3)	20(3)	17(4)
C46	115(6)	131(6)	56(3)	38(4)	27(4)	3(5)
C7	71(4)	114(5)	84(4)	36(4)	17(3)	18(4)
C8	61(3)	131(7)	93(5)	31(4)	19(3)	3(4)
C36	73(3)	94(4)	43(3)	2(3)	1(2)	17(3)
C13	129(6)	63(4)	97(5)	24(3)	43(4)	11(4)
C47	144(7)	101(5)	50(3)	27(3)	-1(4)	3(5)
C16	62(3)	62(3)	41(2)	14.9(19)	14.3(19)	-9(2)
C45	116(5)	127(6)	59(3)	28(4)	36(4)	-14(5)
C39	108(5)	153(8)	55(4)	3(4)	-8(3)	21(5)
C51	173(10)	242(14)	68(5)	40(6)	75(6)	42(9)
C38	158(8)	160(8)	73(4)	64(5)	48(5)	66(7)
C1	113(6)	118(7)	123(6)	46(5)	52(5)	33(5)
C14	145(8)	96(6)	140(7)	41(5)	67(6)	50(6)
C49	136(7)	166(9)	77(4)	42(5)	54(5)	56(6)
C40	186(12)	223(15)	52(4)	28(6)	-1(5)	65(11)
C50	210(13)	340(20)	107(7)	71(10)	77(9)	158(15)
C70	234(16)	330(20)	103(8)	93(11)	38(9)	177(17)
C20	137(7)	162(9)	65(4)	31(5)	11(4)	45(7)
C41	183(11)	217(13)	84(6)	78(7)	-2(7)	57(10)
C42	207(13)	241(17)	80(6)	85(9)	46(7)	112(12)
C52	238(16)	380(30)	114(9)	96(13)	105(10)	159(19)
C55	186(12)	300(20)	125(9)	72(11)	48(9)	120(14)

Table S4. Bond Lengths for DPOTAB.

Atom	Atom	Length/Å	Atom	Atom	Length/Å
C34	C29	1.436(6)	C54	C53	1.372(7)
C34	C21	1.409(7)	C54	C57	1.390(8)
C34	C33	1.421(7)	C53	C60	1.368(7)
C29	C28	1.367(7)	C12	C3	1.442(7)
C29	C30	1.436(7)	C12	C13	1.418(9)
C21	C15	1.500(5)	C3	C2	1.431(9)
C21	C22	1.397(6)	C26	C25	1.349(9)
C28	C27	1.395(7)	C59	C60	1.382(7)
C28	O35	1.402(5)	C59	C58	1.357(8)
O52	C11	1.394(6)	C57	C58	1.351(9)
O52	C53	1.391(6)	C24	C25	1.405(9)
C15	C18	1.389(6)	C44	C45	1.426(8)
C15	C16	1.390(6)	C44	C49	1.381(11)
C27	C22	1.438(6)	C2	C1	1.351(11)
C27	C26	1.421(7)	C48	C47	1.478(9)
C22	C23	1.422(7)	C48	C20	1.346(12)
C4	C5	1.413(7)	C9	C8	1.336(11)
C4	C17	1.490(6)	C37	C36	1.345(10)
C4	C3	1.394(8)	C37	C38	1.351(9)
O35	C36	1.397(7)	C46	C47	1.332(12)
C5	C10	1.436(7)	C46	C45	1.316(12)
C5	C6	1.416(8)	C7	C8	1.412(11)
C18	C17	1.381(6)	C36	C39	1.383(9)
C33	C32	1.358(8)	C13	C14	1.357(12)
C17	C56	1.387(6)	C47	C41	1.466(14)
C43	C19	1.487(6)	C45	C51	1.498(14)
C43	C44	1.423(9)	C39	C40	1.353(16)
C43	C48	1.396(9)	C51	C52	1.336(18)
C10	C11	1.381(9)	C38	C42	1.423(17)
C10	C9	1.438(8)	C1	C14	1.396(13)
C11	C12	1.397(9)	C49	C50	1.383(14)

C23	C24	1.367(8)	C40	C42	1.359(19)
C30	C31	1.348(8)	C50	C52	1.344(16)
C56	C19	1.405(6)	C70	C41	1.332(17)
C19	C16	1.398(6)	C70	C55	1.354(18)
C31	C32	1.393(9)	C20	C55	1.402(16)
C6	C7	1.362(9)			

Table S5. Bond Angles for DPOTAB.

Atom	Atom	Atom	Angle/ [°]	Atom	Atom	Atom	Angle/ [°]
C29	C34	C33	118.2(4)	C54	C53	O52	114.7(4)
C21	C34	C29	119.4(4)	C60	C53	O52	123.8(4)
C21	C34	C33	122.4(4)	C60	C53	C54	121.5(4)
C34	C29	C30	118.5(4)	C11	C12	C3	117.1(5)
C28	C29	C34	119.2(4)	C11	C12	C13	122.6(6)
C28	C29	C30	122.3(4)	C13	C12	C3	120.3(6)
C34	C21	C15	120.2(4)	C4	C3	C12	121.1(5)
C22	C21	C34	120.3(4)	C4	C3	C2	122.4(5)
C22	C21	C15	119.3(4)	C12	C3	C2	116.5(5)
C29	C28	C27	122.9(4)	C25	C26	C27	120.4(5)
C29	C28	O35	119.3(4)	C58	C59	C60	121.1(5)
C27	C28	O35	117.8(4)	C58	C57	C54	120.6(5)
C53	O52	C11	117.8(4)	C53	C60	C59	118.2(5)
C18	C15	C21	117.7(3)	C57	C58	C59	120.1(5)
C18	C15	C16	119.4(4)	C23	C24	C25	120.6(5)
C16	C15	C21	122.9(4)	C45	C44	C43	117.8(7)
C28	C27	C22	118.2(4)	C49	C44	C43	122.6(5)
C28	C27	C26	122.3(4)	C49	C44	C45	119.6(7)
C26	C27	C22	119.6(4)	C26	C25	C24	120.9(5)
C21	C22	C27	120.0(4)	C1	C2	C3	121.1(7)
C21	C22	C23	122.6(4)	C43	C48	C47	117.2(7)
C23	C22	C27	117.5(4)	C20	C48	C43	122.6(6)
C5	C4	C17	120.1(5)	C20	C48	C47	120.3(7)
C3	C4	C5	120.1(4)	C8	C9	C10	121.7(6)
C3	C4	C17	119.9(4)	C38	C37	C36	124.1(7)
C36	O35	C28	117.7(4)	C45	C46	C47	120.4(6)
C4	C5	C10	119.1(5)	C6	C7	C8	120.2(7)
C6	C5	C4	122.5(5)	C9	C8	C7	120.6(6)
C6	C5	C10	118.4(5)	C37	C36	O35	125.2(5)
C17	C18	C15	121.5(4)	C37	C36	C39	119.7(7)
C32	C33	C34	121.1(5)	C39	C36	O35	115.1(7)

C18	C17	C4	120.9(4)	C14	C13	C12	119.9(7)
C18	C17	C56	119.5(4)	C46	C47	C48	121.6(7)
C56	C17	C4	119.6(4)	C46	C47	C41	123.3(8)
C44	C43	C19	118.8(5)	C41	C47	C48	114.9(9)
C48	C43	C19	121.3(5)	C15	C16	C19	119.8(4)
C48	C43	C44	119.5(5)	C44	C45	C51	114.7(8)
C11	C10	C5	119.3(5)	C46	C45	C44	123.3(7)
C11	C10	C9	122.9(5)	C46	C45	C51	121.8(7)
C9	C10	C5	117.7(6)	C40	C39	C36	118.6(11)
O52	C11	C12	118.4(6)	C52	C51	C45	121.6(8)
C10	C11	O52	118.5(5)	C37	C38	C42	115.4(11)
C10	C11	C12	123.1(5)	C2	C1	C14	121.6(8)
C24	C23	C22	121.0(5)	C13	C14	C1	120.6(8)
C31	C30	C29	120.1(5)	C50	C49	C44	122.2(8)
C17	C56	C19	119.9(4)	C39	C40	C42	121.3(10)
C56	C19	C43	117.5(4)	C49	C50	C52	120.2(12)
C16	C19	C43	122.7(4)	C55	C70	C41	121.1(10)
C16	C19	C56	119.8(4)	C48	C20	C55	120.4(9)
C30	C31	C32	121.7(5)	C70	C41	C47	121.6(9)
C7	C6	C5	121.4(6)	C40	C42	C38	120.7(9)
C53	C54	C57	118.4(5)	C51	C52	C50	121.3(11)
C33	C32	C31	120.5(5)	C70	C55	C20	121.7(12)

Table S6. Torsion Angles for DPOTAB.

A	B	C	D	Angle/ [°]	A	B	C	D	Angle/ [°]
C34	C29	C28	C27	-1.8(6)	C10	C9	C8	C7	-0.7(10)
C34	C29	C28	O35	179.7(4)	C11	O52	C53	C54	174.3(5)
C34	C29	C30	C31	0.0(7)	C11	O52	C53	C60	-5.2(8)
C34	C21	C15	C18	85.0(5)	C11	C10	C9	C8	179.9(5)
C34	C21	C15	C16	-93.8(5)	C11	C12	C3	C4	-2.0(7)
C34	C21	C22	C27	-3.8(6)	C11	C12	C3	C2	-179.5(5)
C34	C21	C22	C23	177.3(4)	C11	C12	C13	C14	-178.9(6)
C34	C33	C32	C31	0.9(9)	C23	C24	C25	C26	1.1(11)
C29	C34	C21	C15	-171.3(4)	C30	C29	C28	C27	179.1(4)
C29	C34	C21	C22	3.3(6)	C30	C29	C28	O35	0.6(6)
C29	C34	C33	C32	-0.9(7)	C30	C31	C32	C33	-0.5(9)
C29	C28	C27	C22	1.3(7)	C56	C19	C16	C15	-3.6(8)
C29	C28	C27	C26	-179.1(5)	C19	C43	C44	C45	-177.6(5)
C29	C28	O35	C36	-97.4(5)	C19	C43	C44	C49	2.9(10)
C29	C30	C31	C32	0.1(9)	C19	C43	C48	C47	177.7(6)
C21	C34	C29	C28	-0.6(6)	C19	C43	C48	C20	-2.5(11)
C21	C34	C29	C30	178.6(4)	C6	C5	C10	C11	-178.8(4)
C21	C34	C33	C32	-179.0(5)	C6	C5	C10	C9	2.1(6)
C21	C15	C18	C17	179.9(4)	C6	C7	C8	C9	1.4(10)
C21	C15	C16	C19	-178.3(4)	C54	C53	C60	C59	-0.2(9)
C21	C22	C23	C24	179.0(5)	C54	C57	C58	C59	1.5(10)
C28	C29	C30	C31	179.1(5)	C53	O52	C11	C10	96.2(6)
C28	C27	C22	C21	1.5(6)	C53	O52	C11	C12	-85.0(6)
C28	C27	C22	C23	-179.6(4)	C53	C54	C57	C58	-1.3(10)
C28	C27	C26	C25	179.5(5)	C12	C3	C2	C1	-1.2(9)
C28	O35	C36	C37	12.2(8)	C12	C13	C14	C1	-1.8(13)
C28	O35	C36	C39	-167.8(5)	C3	C4	C5	C10	-3.6(6)
O52	C11	C12	C3	-178.6(4)	C3	C4	C5	C6	177.0(4)
O52	C11	C12	C13	-0.1(8)	C3	C4	C17	C18	91.2(6)
O52	C53	C60	C59	179.2(5)	C3	C4	C17	C56	-89.7(6)
C15	C21	C22	C27	170.9(4)	C3	C12	C13	C14	-0.4(10)

C15 C21 C22 C23	-8.0(6)	C3 C2 C1 C14	-1.0(13)
C15 C18 C17 C4	179.2(5)	C26 C27 C22 C21	-178.1(4)
C15 C18 C17 C56	0.1(8)	C26 C27 C22 C23	0.8(7)
C27 C28 O35 C36	84.0(5)	C57 C54 C53 O52	-178.9(6)
C27 C22 C23 C24	0.2(8)	C57 C54 C53 C60	0.6(9)
C27 C26 C25 C24	-0.1(11)	C60 C59 C58 C57	-1.1(9)
C22 C21 C15 C18	-89.7(5)	C58 C59 C60 C53	0.5(8)
C22 C21 C15 C16	91.5(6)	C44 C43 C19 C56	84.2(7)
C22 C27 C26 C25	-0.8(8)	C44 C43 C19 C16	-96.4(7)
C22 C23 C24 C25	-1.1(10)	C44 C43 C48 C47	4.6(9)
C4 C5 C10 C11	1.9(6)	C44 C43 C48 C20	-175.6(7)
C4 C5 C10 C9	-177.2(4)	C44 C45 C51 C52	-1.6(19)
C4 C5 C6 C7	177.8(5)	C44 C49 C50 C52	4(3)
C4 C17 C56 C19	-179.8(5)	C2 C1 C14 C13	2.6(15)
C4 C3 C2 C1	-178.8(6)	C48 C43 C19 C56	-89.0(7)
O35 C28 C27 C22	179.8(4)	C48 C43 C19 C16	90.4(7)
O35 C28 C27 C26	-0.6(7)	C48 C43 C44 C45	-4.3(9)
O35 C36 C39 C40	-179.6(8)	C48 C43 C44 C49	176.2(7)
C5 C4 C17 C18	-89.4(6)	C48 C47 C41 C70	1(2)
C5 C4 C17 C56	89.6(6)	C48 C20 C55 C70	-2(3)
C5 C4 C3 C12	3.7(7)	C9 C10 C11 O52	-2.4(7)
C5 C4 C3 C2	-178.9(4)	C9 C10 C11 C12	178.9(4)
C5 C10 C11 O52	178.6(4)	C37 C36 C39 C40	0.4(12)
C5 C10 C11 C12	-0.2(7)	C37 C38 C42 C40	-2.7(17)
C5 C10 C9 C8	-1.1(8)	C46 C47 C41 C70	-174.7(14)
C5 C6 C7 C8	-0.3(9)	C46 C45 C51 C52	174.1(15)
C18 C15 C16 C19	2.9(7)	C36 C37 C38 C42	2.4(12)
C18 C17 C56 C19	-0.7(8)	C36 C39 C40 C42	-0.8(18)
C33 C34 C29 C28	-178.7(4)	C13 C12 C3 C4	179.5(5)
C33 C34 C29 C30	0.4(6)	C13 C12 C3 C2	1.9(8)
C33 C34 C21 C15	6.8(6)	C47 C48 C20 C55	-0.4(17)
C33 C34 C21 C22	-178.6(4)	C47 C46 C45 C44	-2.6(13)
C17 C4 C5 C10	177.0(4)	C47 C46 C45 C51	-178.0(9)

C17 C4 C5 C6	-2.3(6)	C16 C15 C18 C17	-1.2(7)
C17 C4 C3 C12	-176.9(4)	C45 C44 C49 C50	0.6(17)
C17 C4 C3 C2	0.5(7)	C45 C46 C47 C48	2.9(13)
C17 C56 C19 C43	-178.1(5)	C45 C46 C47 C41	178.0(10)
C17 C56 C19 C16	2.5(8)	C45 C51 C52 C50	6(3)
C43 C19 C16 C15	177.0(5)	C39 C40 C42 C38	2(2)
C43 C44 C45 C46	3.3(11)	C38 C37 C36 O35	178.7(6)
C43 C44 C45 C51	179.0(7)	C38 C37 C36 C39	-1.3(11)
C43 C44 C49 C50	180.0(12)	C49 C44 C45 C46	-177.2(8)
C43 C48 C47 C46	-3.9(11)	C49 C44 C45 C51	-1.6(12)
C43 C48 C47 C41	-179.4(8)	C49 C50 C52 C51	-7(3)
C43 C48 C20 C55	179.8(11)	C20 C48 C47 C46	176.3(9)
C10 C5 C6 C7	-1.5(7)	C20 C48 C47 C41	0.8(13)
C10 C11 C12 C3	0.2(7)	C41 C70 C55 C20	3(3)
C10 C11 C12 C13	178.7(5)	C55 C70 C41 C47	-3(3)

Table S7. Hydrogen Atom Coordinates ($\text{\AA} \times 10^4$) and Isotropic Displacement Parameters ($\text{\AA}^2 \times 10^3$) for DPOTAB.

Atom	x	y	z	U(eq)
H18	2373.28	3149.91	1091.57	64
H33	3240.08	1265.95	1251.84	74
H23	-673.69	2693.31	1341.22	80
H30	1127.93	-352.13	-1531.48	78
H56	3510.42	3889.82	3641.91	73
H31	3160.91	-512.76	-864.18	91
H6	5329.34	3221.43	2430.77	84
H54	7059.71	7955.09	2018.04	91
H32	4210.84	277.37	520.89	92
H26	-2705.77	1092.54	-1462.76	88
H59	4679.03	6076.21	-546.11	81
H57	6910.58	8301.89	743.09	106
H60	4776.18	5707.58	706.14	78
H58	5770.51	7349.27	-521.65	95
H24	-2740.55	2823.87	665.19	105
H25	-3736.1	2037.79	-741.99	103
H2	1477.56	4740.97	2398.73	106
H9	7682.38	5646.75	2228.01	98
H37	400.38	1614.86	-1775.01	103
H46	2271.17	2528.3	6177.08	119
H7	7424.38	3236.75	2381.84	107
H8	8584.09	4454.32	2252.94	116
H13	3916.73	7194.3	2290.03	113
H16	1163.21	1626.28	2375.13	68
H39	-2336.55	-317.44	-3277.78	139
H51	423.61	3337.11	6136.21	184
H38	484.73	2173.82	-2878.49	143
H1	613.06	5954.83	2372.97	134
H14	1834.85	7192.82	2370.9	142
H49	472.31	3526.31	3471.65	142

H40	-2337.82	223.34	-4404.43	192
H50	-990.81	4126.2	4121.84	245
H70	5673.8	1218.78	5666.35	253
H20	4155.14	1926.72	3565.82	148
H41	4130.48	1703.2	6247.51	193
H42	-1024.81	1465.75	-4228.24	195
H52	-837.94	4148.44	5490.21	266
H55	5645.83	1259.54	4330.62	233

Table S8. Spin-orbit coupling matrix elements

SOC	DPOTAB	DPOTABCN
$\langle S_1 \hat{H}_{\text{SOC}} T_1 \rangle$	0.062 cm ⁻¹	0.088 cm ⁻¹
$\langle S_1 \hat{H}_{\text{SOC}} T_2 \rangle$	0.162 cm ⁻¹	0.345 cm ⁻¹
$\langle S_1 \hat{H}_{\text{SOC}} T_3 \rangle$	0.301 cm ⁻¹	0.145 cm ⁻¹
$\langle S_1 \hat{H}_{\text{SOC}} T_4 \rangle$	0.080 cm ⁻¹	0.016 cm ⁻¹
$\langle S_1 \hat{H}_{\text{SOC}} T_5 \rangle$	0.332 cm ⁻¹	0.272 cm ⁻¹
$\langle S_1 \hat{H}_{\text{SOC}} T_6 \rangle$	0.128 cm ⁻¹	0.176 cm ⁻¹

Thermal and electronic characterization

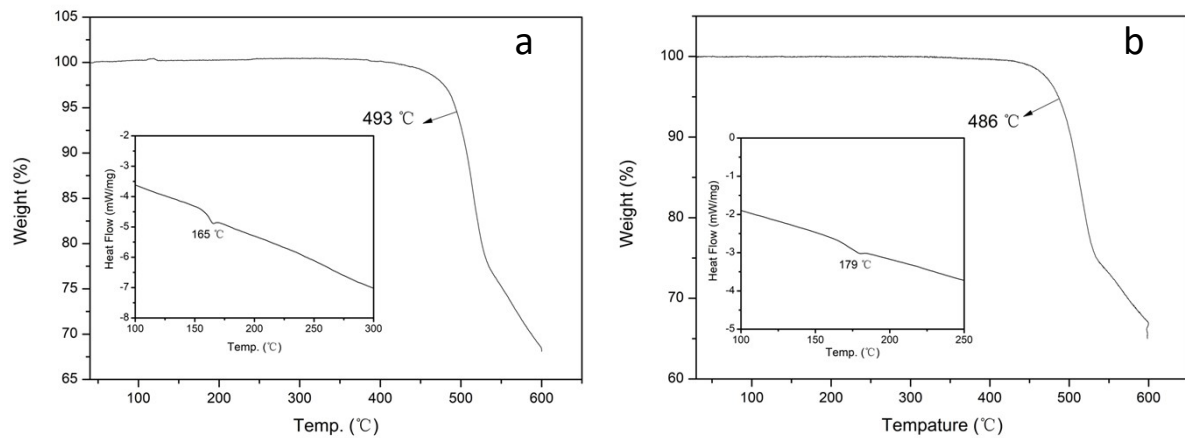


Figure S2. Thermal analysis of (a) DPOTAB and (b) DPOTABCN measured using TGA and DSC.

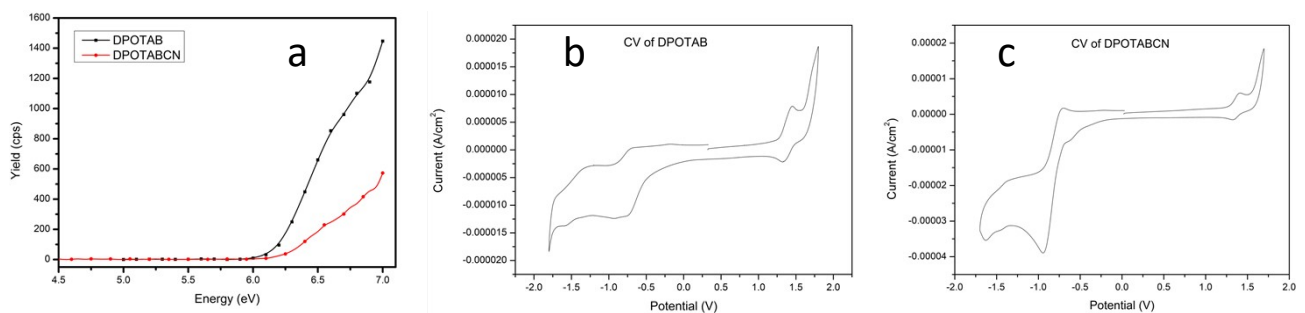


Figure S3. Ionization potential analysis of DPOTAB and DPOTABCN measured using photoelectron spectroscopy (a), and cyclic voltammetry of DPOTAB (b) and DPOTABCN (c).

PLQE calculations

UV-visible absorption and PL emission spectra were recorded for cyclohexane solutions at room temperature in a cuvette having a 10 mm path length. The excitation wavelength for PL emission spectra was 372 nm. The PL (fluorescence in this case) quantum yields of DPOTAB and DPOTABCN were calculated using a solution of the 9,10-DPA standard having a known fluorescence quantum yield, according to the equation (subscripts X and ST denote sample and standard, respectively)

$$\Phi_X = \Phi_{ST} (M_X/M_{ST}) (\eta^2 X / \eta^2 ST)$$

where Φ is the fluorescence quantum yield (fluorescence quantum *efficiency* is Φ stated as a percentage), M is the slope of the best-fit straight line in a plot of integrated fluorescence intensity as a function of the fraction of light absorbed by the fluorescing species at the excitation wavelength, and η the refractive index of the solvent. For solutions having an absorbances up to around 0.1 at the excitation wavelength, such as in the present work, absorbance values can be used in the calculation of M instead of the fraction of light absorbed. The literature values for the fluorescence quantum yield of 9,10-DPA, Φ_{ST} , in cyclohexane solution with and without de-oxygenation are 0.91 and 0.70, respectively.¹ In the present work, solution de-oxygenation was achieved by bubbling with N₂ gas.

From the results shown in **Figure S4**, the room-temperature fluorescence quantum yield/efficiency of **DPOTAB** in cyclohexane at room temperature is obtained as follows:

$$\text{Air-equilibrated: } \Phi_{DPOTAB} = 0.70 \times (182.81 \div 188.02) = 0.68 \text{ (PLQE = 68%)}$$

$$\text{De-oxygenated: } \Phi_{DPOTAB} = 0.91 \times (197.34 \div 198.45) = 0.90 \text{ (PLQE = 90%)}$$

From the results shown in **Figure S5**, the fluorescence quantum yield/efficiency of **DPOTABCN** in cyclohexane at room temperature is obtained as follows:

$$\text{Air-equilibrated: } \Phi_{DPOTABCN} = 0.70 \times (246,486.873 \div 287,295.068) = 0.60 \text{ (PLQE = 60%)}$$

$$\text{De-oxygenated: } \Phi_{DPOTABCN} = 0.91 \times (257,204.948 \div 309,224.028) = 0.76 \text{ (PLQE = 76%)}$$

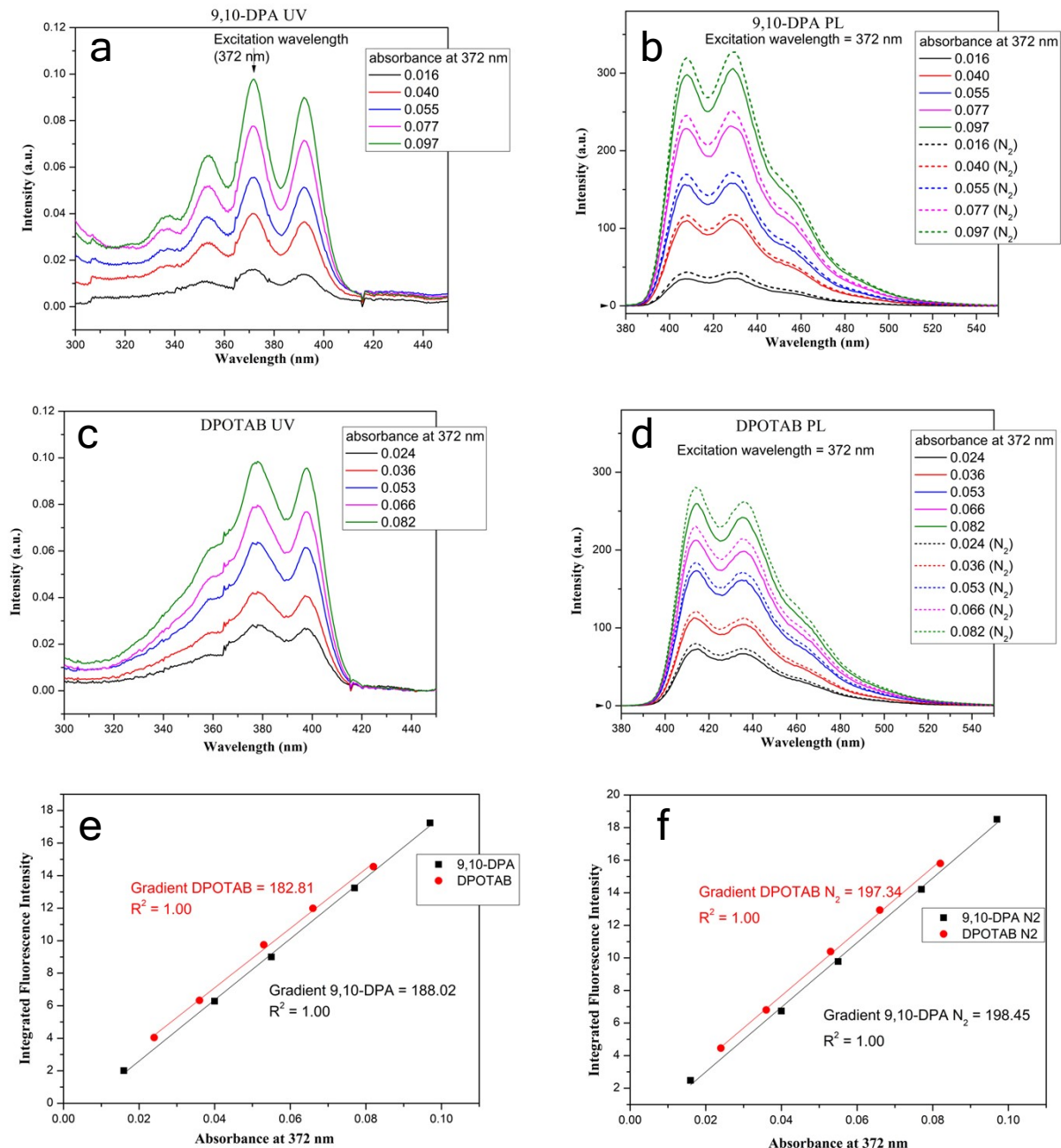


Figure S4. Calculation of PL quantum yield of DPOTAB in cyclohexane solution: (a) UV absorption of 9,10-DPA, (b) PL of 9,10-DPA excited at 372 nm without and with N₂ bubbling, (c) UV absorption of DPOTAB, (d) PL of DPOTAB excited at 372 nm without and with N₂ bubbling, (e) Calibration curves of integrated fluorescence intensity (area) as a function of absorbance for 9,10-DPA and DPOTAB without N₂ bubbling, (f) Calibration curves of integrated fluorescence intensity (area) as a function of absorbance for 9,10-DPA and DPOTAB with N₂ bubbling.

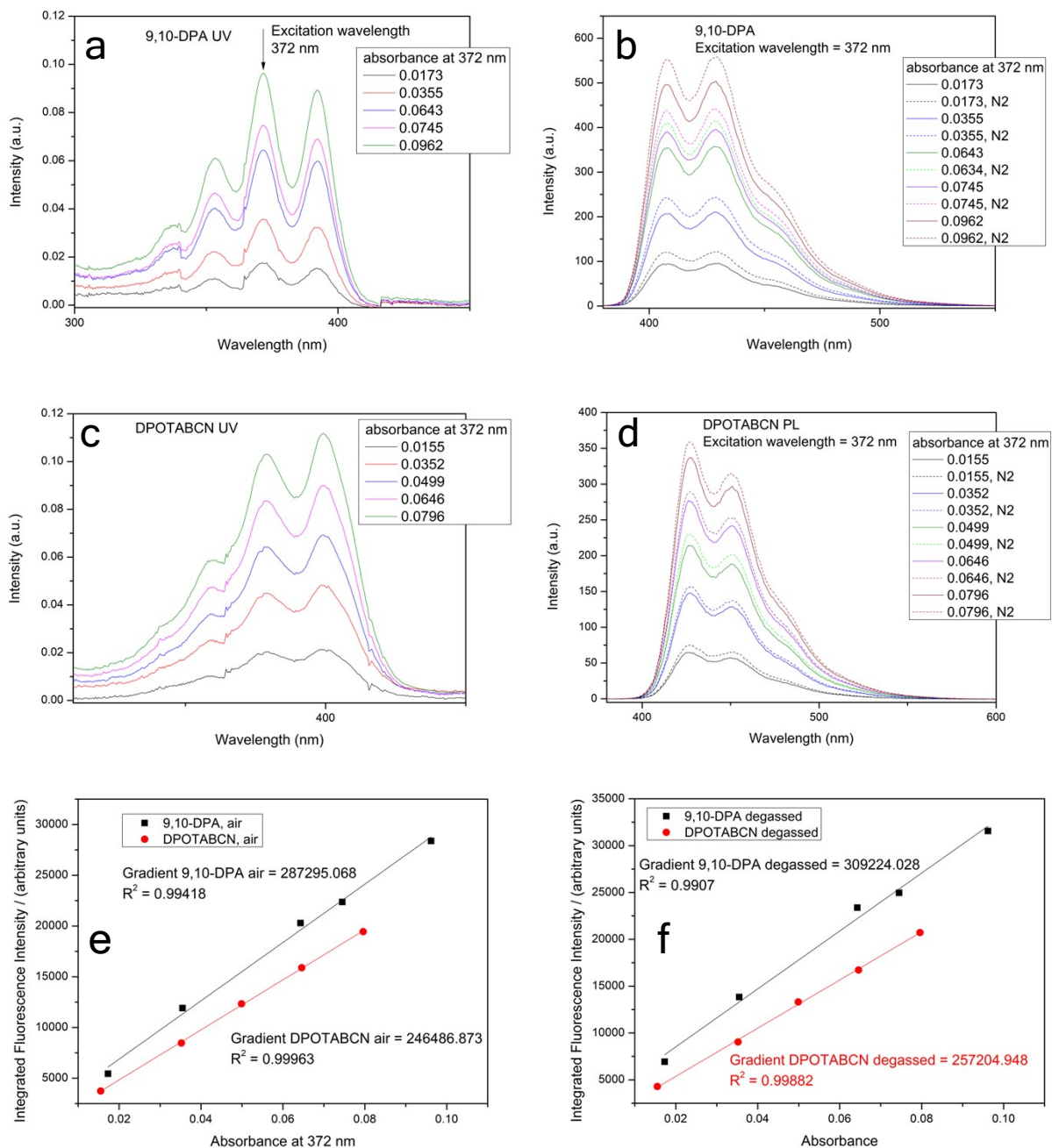


Figure S5. Calculation of PL quantum yield of DPOTABCN in cyclohexane solution: (a) UV absorption of 9,10-DPA, (b) PL of 9,10-DPA excited at 372 nm without and with N₂ bubbling, (c) UV absorption of DPOTABCN, (d) PL of DPOTABCN excited at 372 nm without and with N₂ bubbling, (e) Calibration curves of integrated fluorescence intensity (area) as a function of absorbance for 9,10-DPA and DPOTABCN without N₂ bubbling, (f) Calibration curves of integrated fluorescence intensity (area) as a function of absorbance for 9,10-DPA and DPOTABCN with N₂ bubbling.

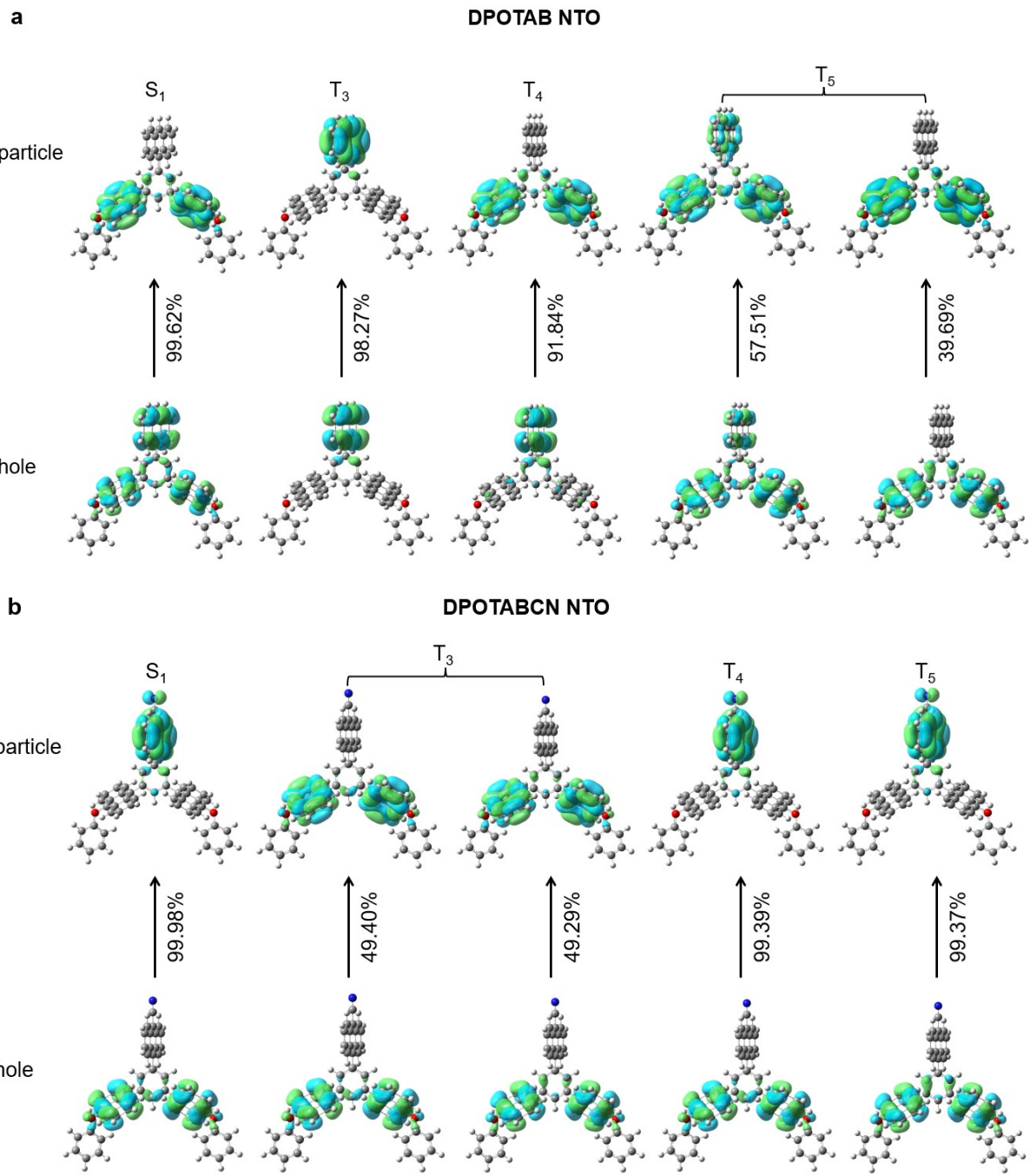


Figure S6. Calculated NTOs of (a) DPOTAB and (b) DPOTABCN.

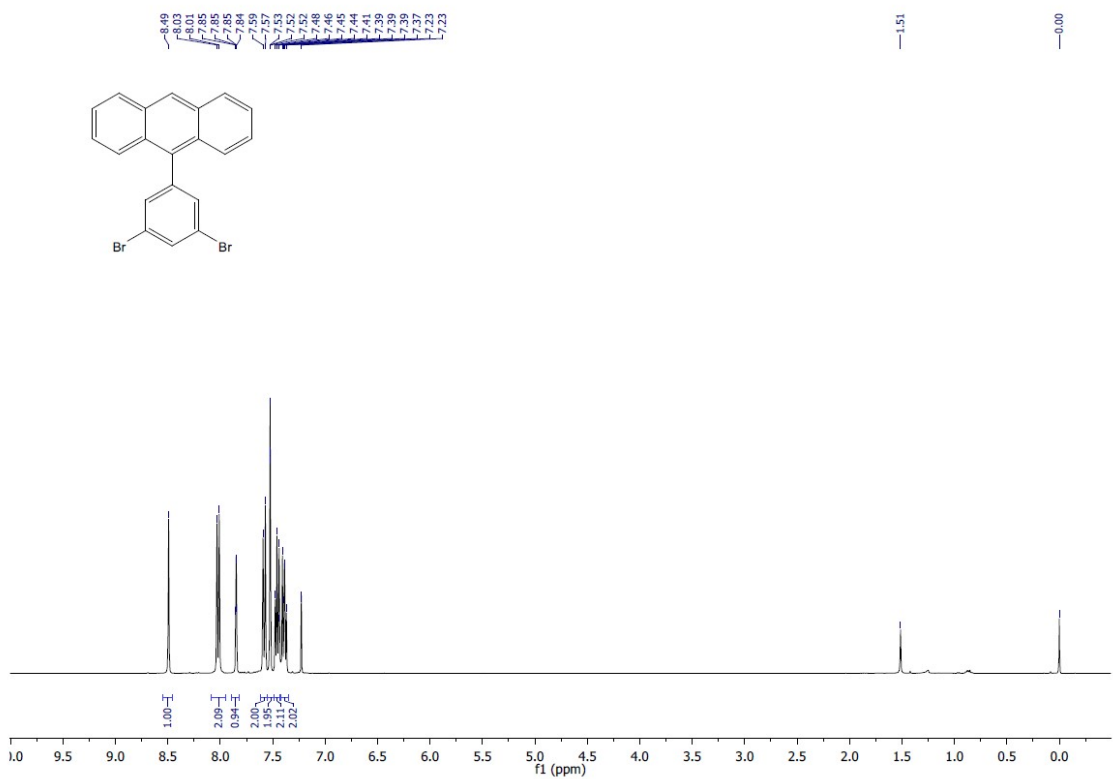


Fig. S7. ¹H NMR spectrum of compound 1.

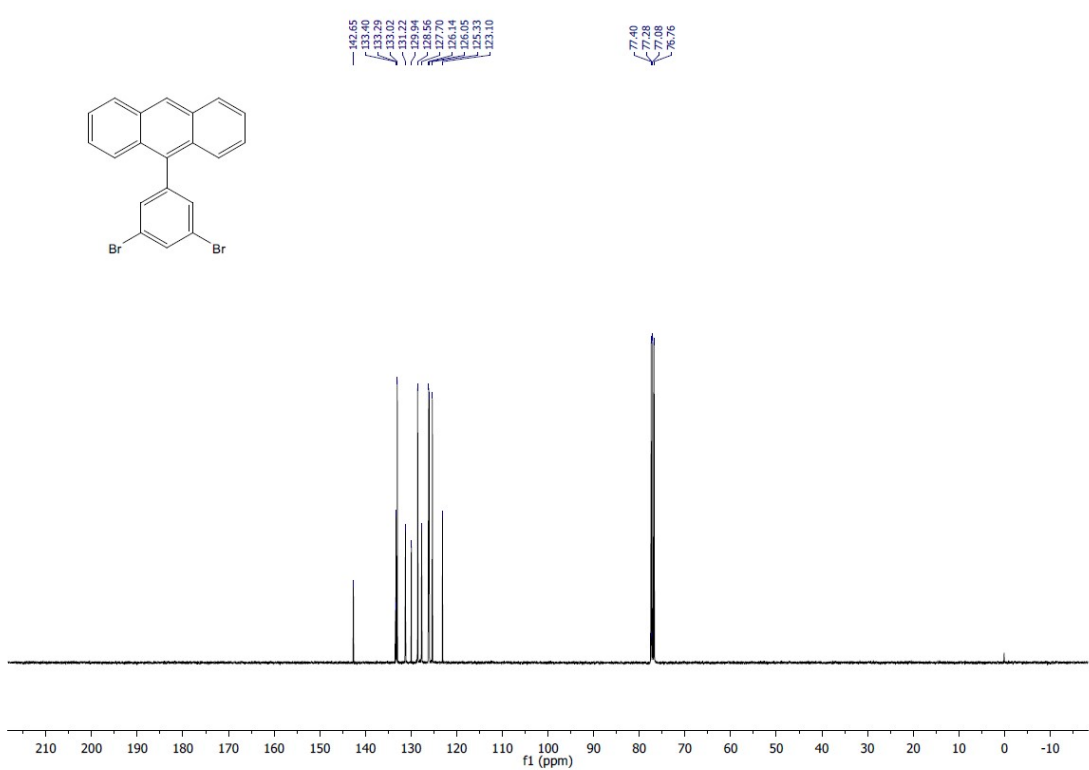


Fig. S8. ¹³C NMR spectrum of compound 1.

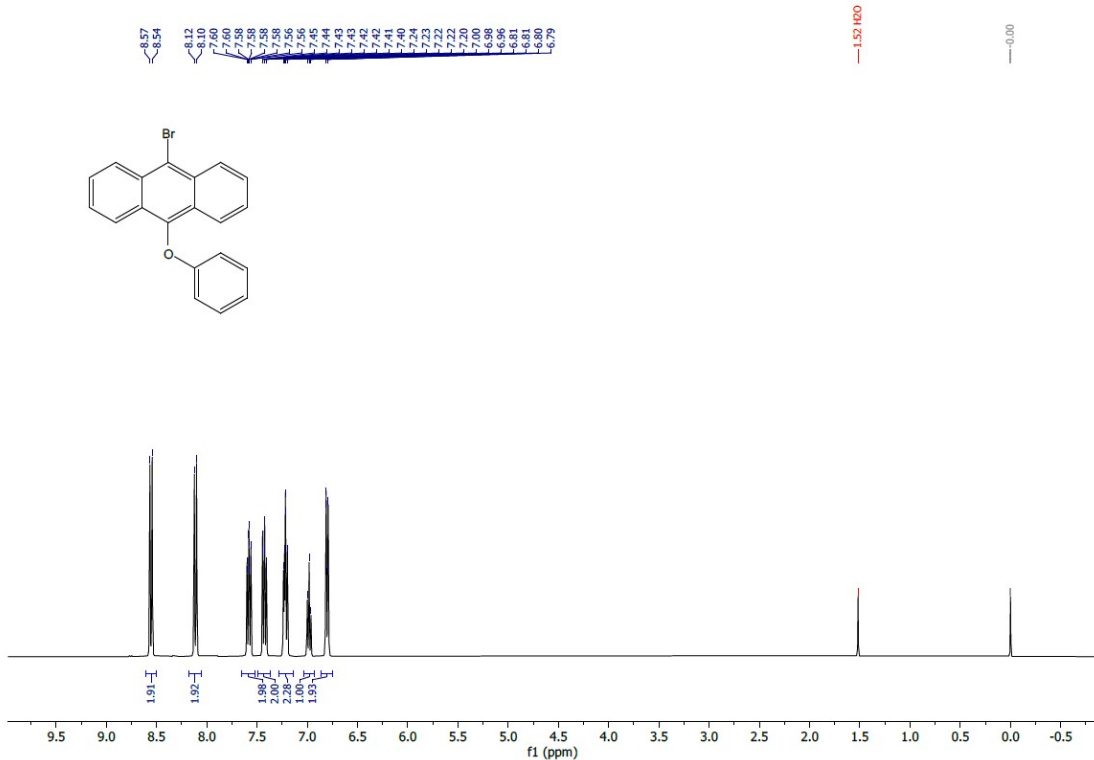


Fig. S9. ^1H NMR spectrum of compound 2.

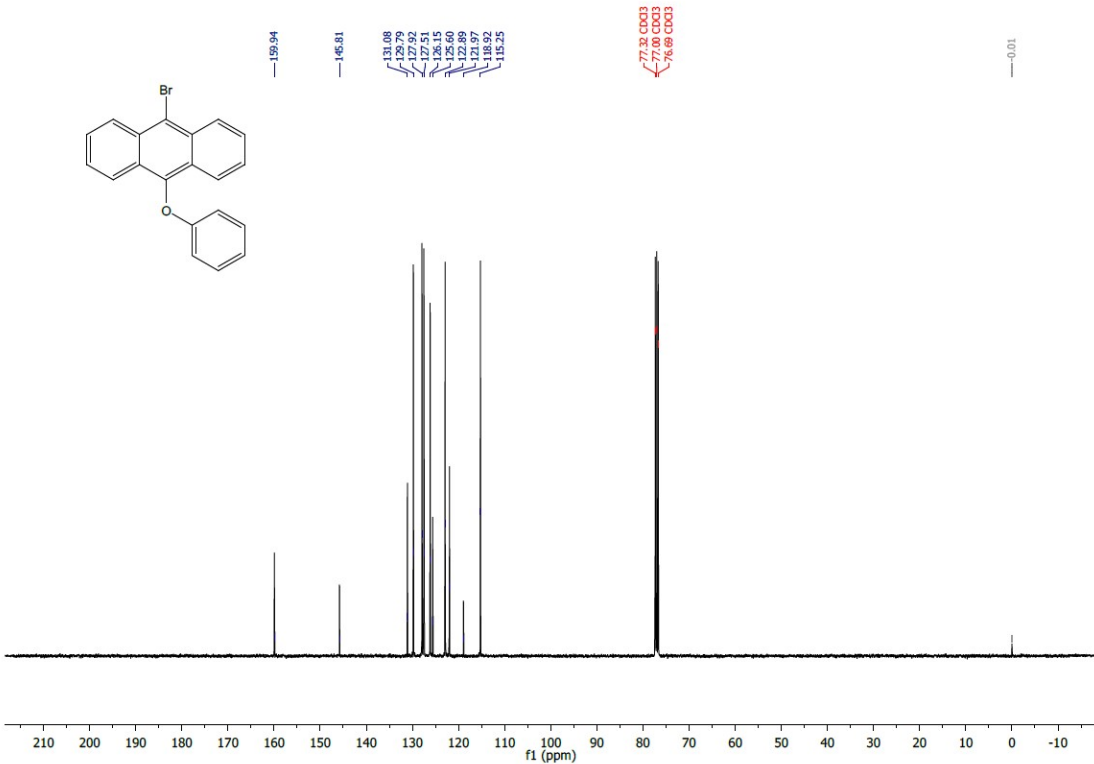


Fig. S10. ^{13}C NMR spectrum of compound 2.

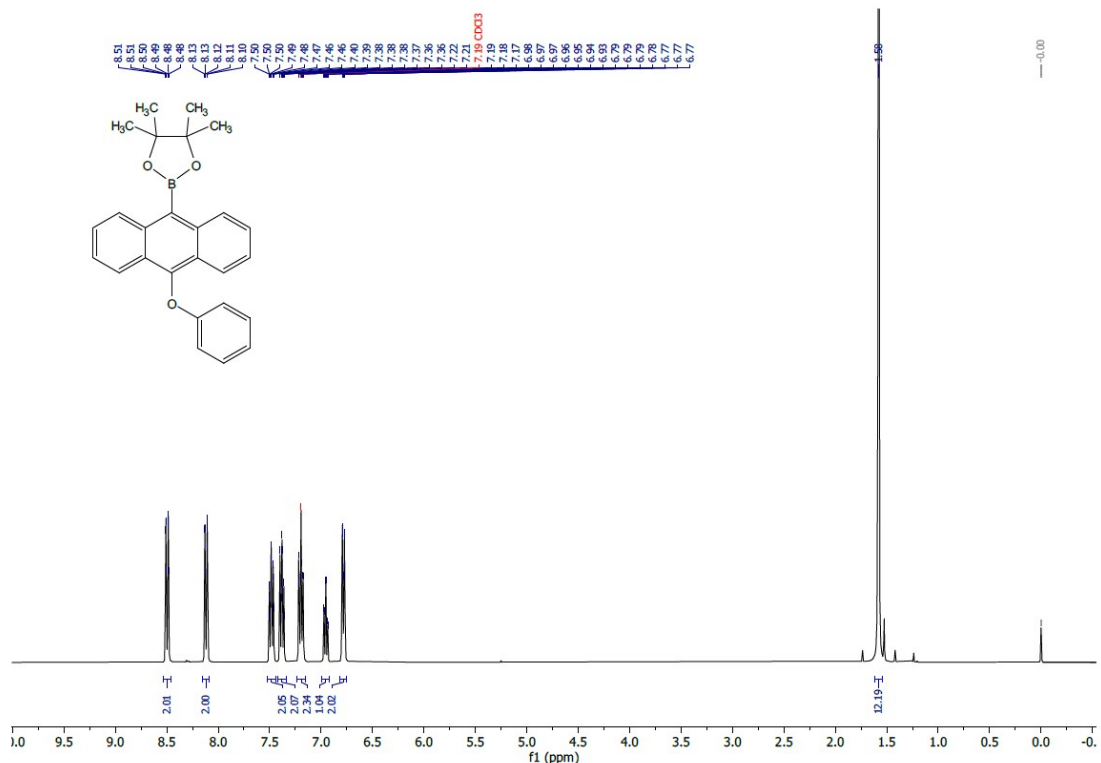


Fig. S11. ^1H NMR spectrum of compound 3.

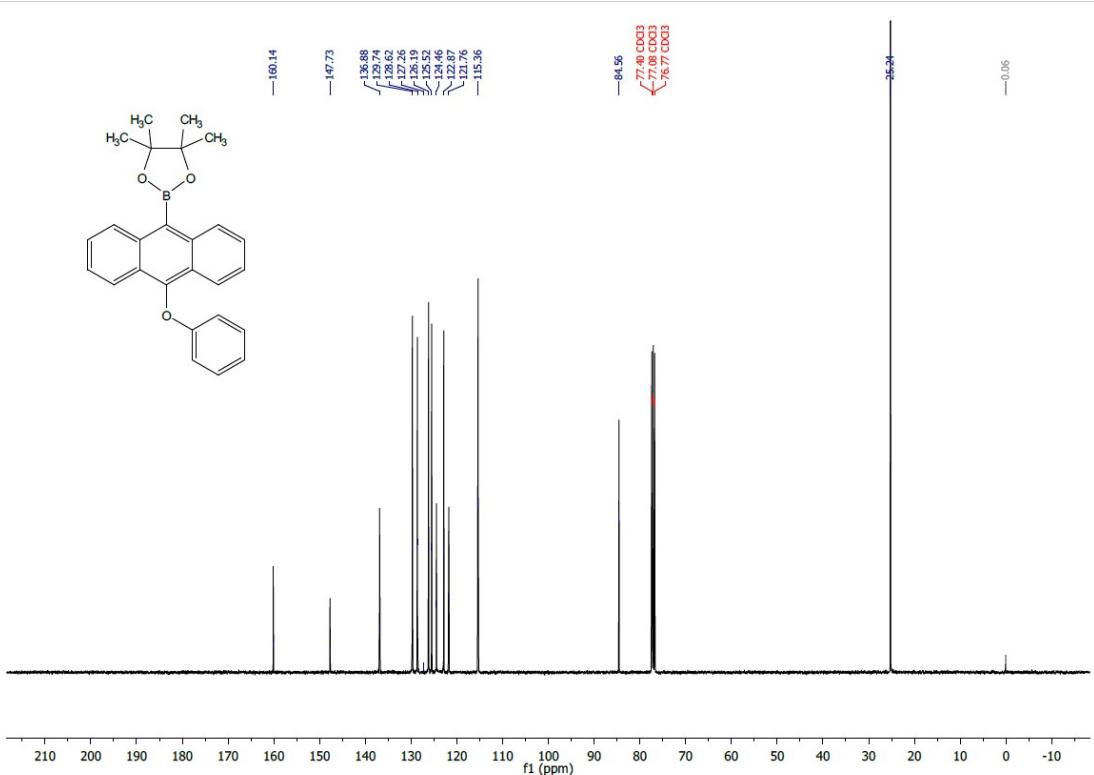


Fig. S12. ^{13}C NMR spectrum of compound **3**.

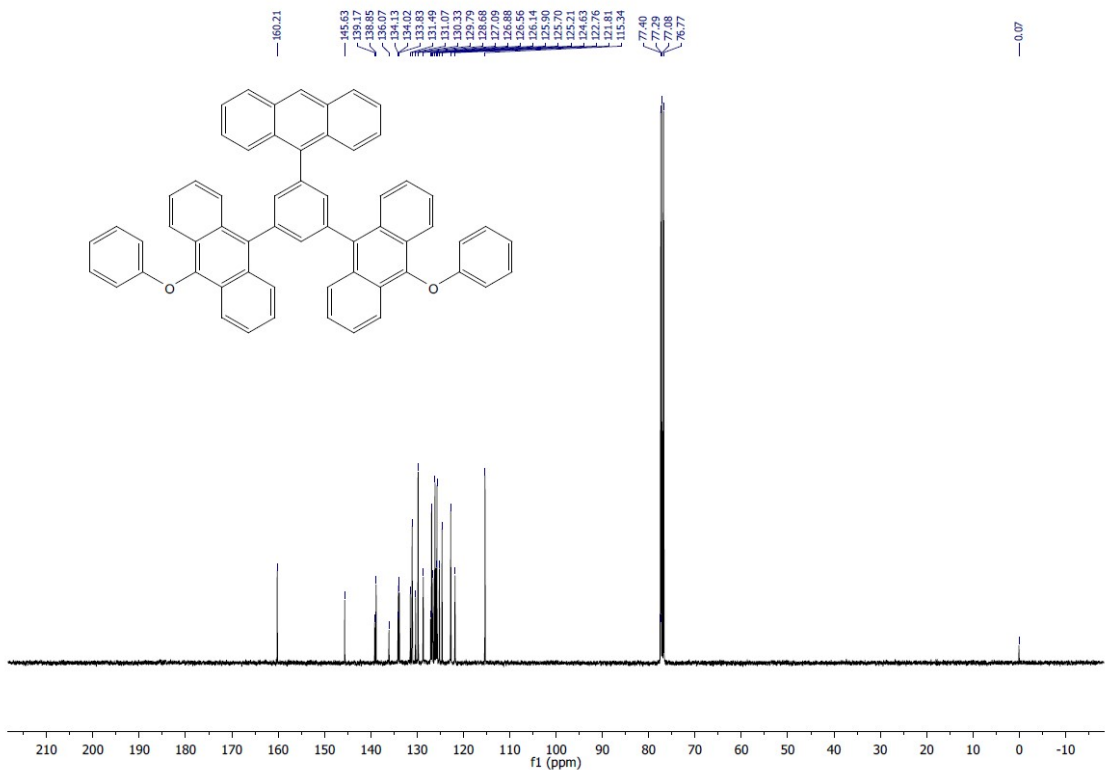
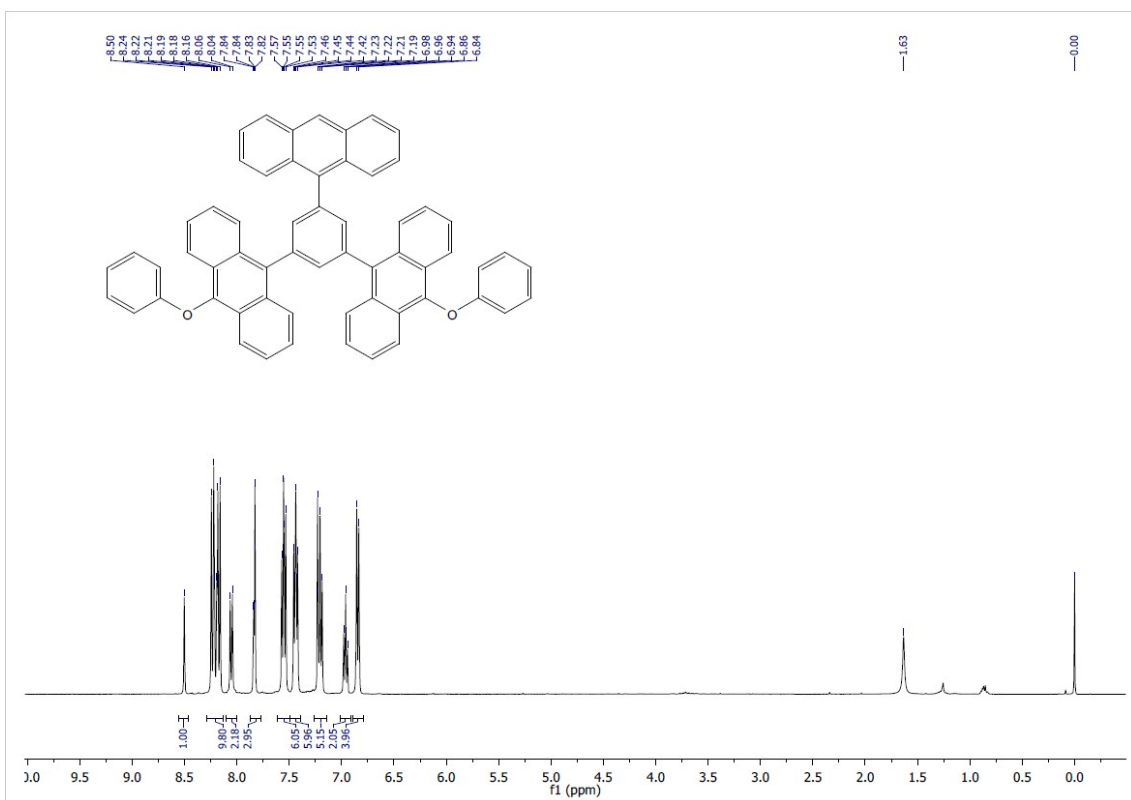


Fig. S14. ^{13}C NMR spectrum of compound DPOTAB.

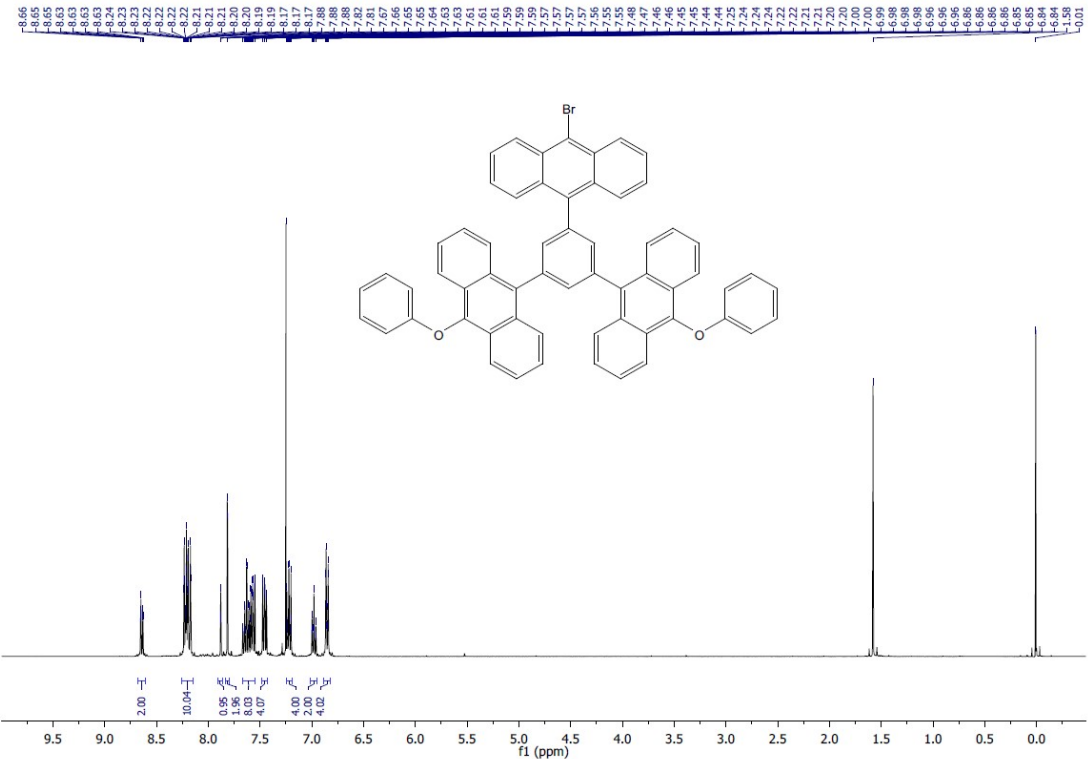


Fig. S15. ^1H NMR spectrum of compound 4.

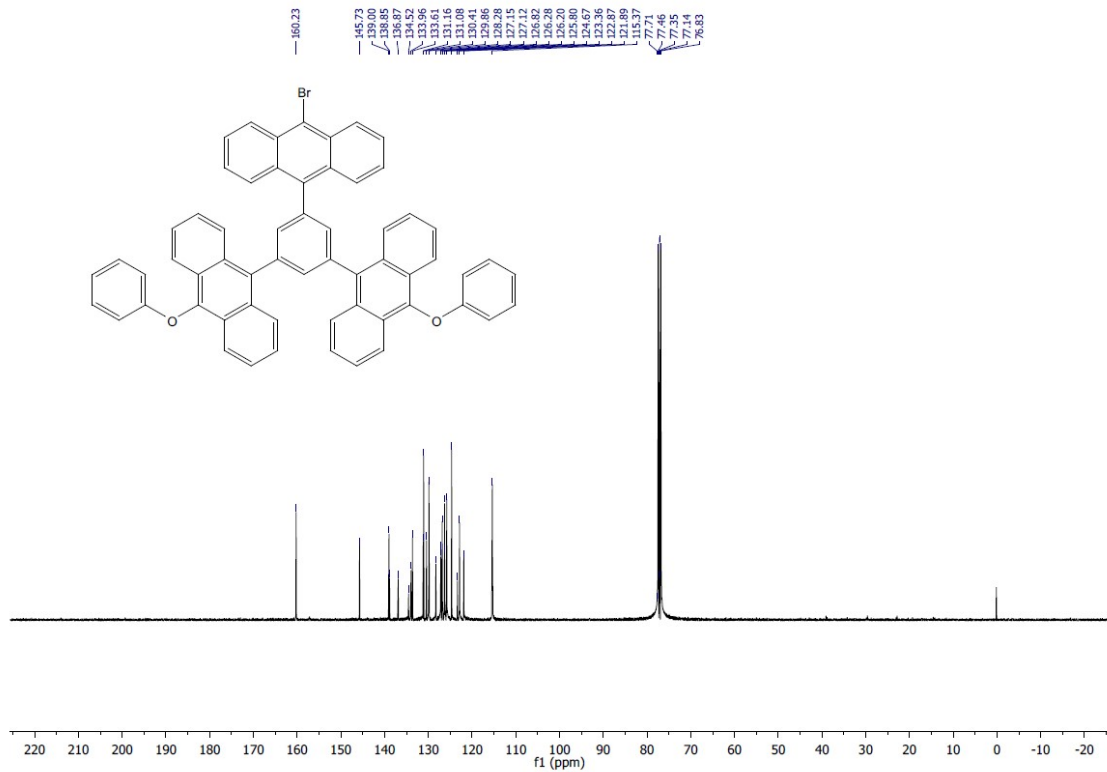


Fig. S16. ^{13}C NMR spectrum of compound 4.

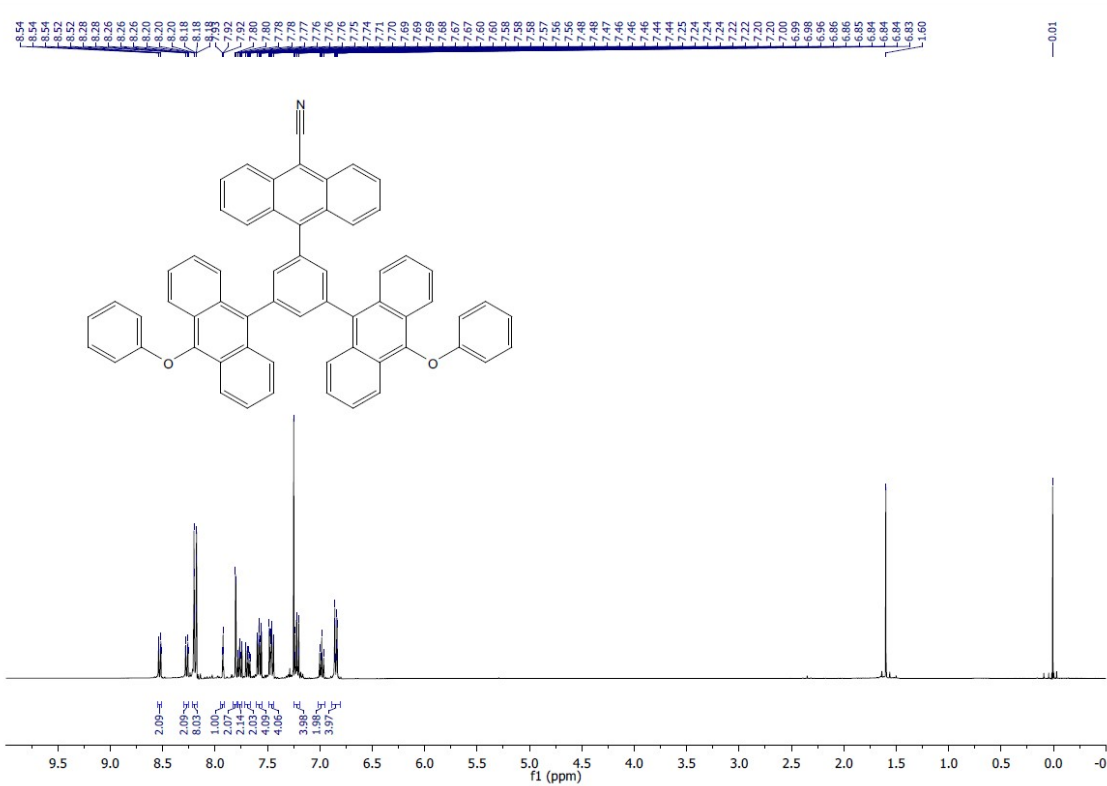


Fig. S17. ^1H NMR spectrum of compound **DPOTABCN**.

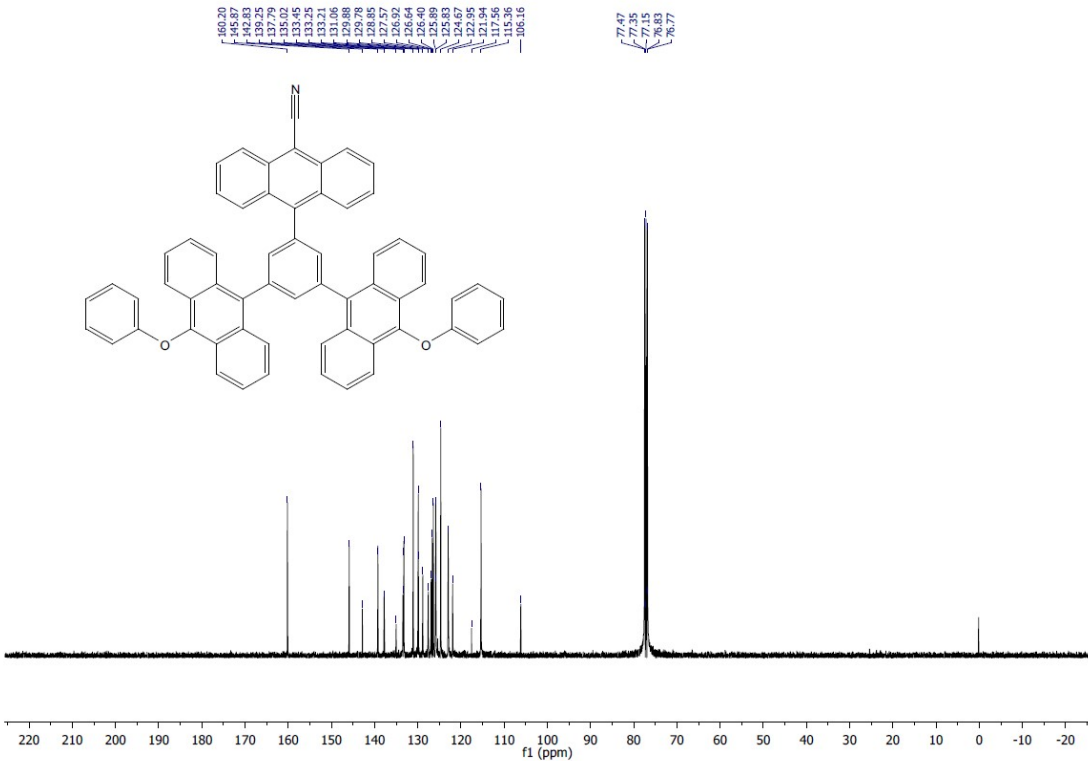


Fig. S18. ^{13}C NMR spectrum of compound **DPOTABCN**.

References

- (1) Rurack, K., Fluorescence Quantum Yields: Methods of Determination and Standards. In *Standardization and Quality Assurance in Fluorescence Measurements I: Techniques*, Resch-Genger, U., Ed. Springer Berlin Heidelberg: Berlin, Heidelberg, 2008; pp 101-145.